Published in final edited form as:
Kidney Int. 2020 March 01; 97(3): 609–614. doi:10.1016/j.kint.2019.08.029.

Collagen-specific molecular imaging of renal fibrosis

Maike Baues[#1], **Barbara M Klinkhammer**[#2,3], **Josef Ehling**[1,2], **Felix Gremse**[1], **Marc A. M. J. van Zandvoort**[4], **Chris P. M. Reutelingsperger**[5], **Christoph Daniel**[6], **Kerstin Amann**[6], **Janka Bábíčková**[3,7,8], **Fabian Kiessling**[1], **Jürgen Floege**[3], **Twan Lammers**[1,9,10,*], **Peter Boor**[2,3,11,*]

[1]Institute for Experimental Molecular Imaging, RWTH Aachen University Hospital, Aachen, Germany [2]Institute of Pathology, RWTH Aachen University Hospital, Aachen, Germany [3]Department of Nephrology and Immunology, RWTH Aachen University Hospital, Aachen, Germany [4]Department of Biochemistry, University Hospital Maastricht (azM), Maastricht, The Netherlands [5]Department of Pathology, Electron Microscopy Unit, University of Maastricht, Maastricht, The Netherlands [6]Institute of Pathology, University Erlangen, Erlangen, Germany [7]Institute of Molecular Biomedicine, Comenius University, Bratislava, Slovakia [8]Department of Clinical Medicine, University of Bergen, Bergen, Norway [9]Department of Pharmaceutics, Utrecht University, The Netherlands [10]Department of Targeted Therapeutics, University of Twente, Enschede, The Netherlands [11]Electron Microscopy Facility, RWTH Aachen University Hospital, Aachen, Germany

[#] These authors contributed equally to this work.

Abstract

Pathological deposition of collagen is a hallmark of renal fibrosis. We employed multimodal optical imaging to visualize and quantify collagen deposition in murine models of kidney fibrosis using the collagen-binding agent CNA35. For *in vivo* imaging, we used hybrid computed tomography-fluorescence molecular tomography (CT-FMT) and CNA35 labeled with the near-infrared fluorophore Cy7. Upon i.v. injection, CNA35-Cy7 accumulation was significantly higher in fibrotic kidneys compared to non-fibrotic kidneys. This difference was not detected for a non-specific scrambled version of CNA35-Cy7. *Ex vivo,* on kidney sections of animals and patients with renal fibrosis, CNA35-FITC co-localized with scar collagen type I and III, but not with the basement membrane collagen type IV. Upon i.v. injection, CNA35-FITC bound to both interstitial and perivascular fibrotic areas. In line with this perivascular accumulation, we observed significant perivascular fibrosis in animal models and patients using computer-based morphometry quantification. In conclusion, molecular imaging of collagen using CNA35 enables specific non-invasive quantification of renal fibrosis. Collagen imaging revealed significant perivascular fibrosis as a consistent component next to the more commonly assessed interstitial fibrosis. Our results lay the basis for further probe and protocol optimization towards the clinical translation of molecular imaging of kidney fibrosis.

[*]Address correspondence to: Peter Boor, MD, PhD, Institute of Pathology, RWTH Aachen University Hospital, Pauwelsstrasse 30, 52074 Aachen, Germany, Phone: +49 241 80 85227, Fax: +49 241 80 82446, pboor@ukaachen.de; Twan Lammers, PhD, DSc, Institute for Experimental Molecular Imaging, RWTH Aachen University Hospital, Forckenbeckstrasse 55, 52074 Aachen, Germany, Phone: +49 241 80 36681, Fax: +49 241 80 3380116, tlammers@ukaachen.de.

Disclosure: No conflicts of interest to disclose.

Europe PMC Funders Author Manuscripts

Keywords

Molecular imaging; kidney fibrosis; chronic kidney disease (CKD); biomarker; collagen; extracellular matrix (ECM)

Introduction

Renal fibrosis is a common finding in chronic kidney diseases (CKD), independent of the underlying disease etiology.[1] Fibrosis is characterized by pathological production and accumulation of extracellular matrix (ECM) in the renal interstitium, mainly comprising collagens. Although multiple anti-fibrotic targets have been identified in preclinical research, no targeted therapeutics have made it into clinical routine. A potential reason for this poor translation is the lack of non-invasively accessible fibrosis-specific study endpoints in clinical trials.[2,3] We recently showed that elastin-specific magnetic resonance imaging (MRI) enables non-invasive staging and treatment monitoring of renal fibrosis.[4] Here, we describe a method for the visualization and quantification of the most common extracellular matrix component in fibrotic kidneys, i.e. collagen. We employed the collagen-binding protein fragment CNA35, which binds to fibril-forming collagens, but not to other extracellular matrix components (such as laminin, elastin and fibronectin), and which has already been shown to hold promise for visualizing cardiovascular fibrosis.[5–7] Using optical imaging, we demonstrate in two murine models (unilateral ureteral obstruction (UUO) and ischemia-reperfusion injury (I/R)) that fluorophore-labeled CNA35 can specifically and non-invasively detect collagen deposition in renal fibrosis.

Results

Optical imaging of CNA35 accumulation in fibrotic kidneys

Hybrid computed tomography-fluorescence molecular tomography (CT-FMT) imaging showed significantly higher CNA35 accumulation in kidneys with I/R-induced firbosis compared to contralateral healthy kidneys at 24, 48 and 72 h after i.v. injection of 1 nmol of CNA35-Cy7 (Fig. 1a,b). Off-target accumulation of CNA35 was observed in liver and spleen, which likely results from capture and clearance by the reticuloendothelial system (Supp. Fig. S1a). Clearance of CNA35 from fibrotic kidneys was substantially slower than from healthy kidneys. Similar findings were observed after i.v. injection of 5 nmol CNA35-Cy7 (Supp. Fig. S1b,c). *Ex vivo* fluorescence reflectance imaging (FRI) confirmed the *in vivo* findings, showing significantly increased probe retention in fibrotic vs. healthy kidneys, for both 1 and 5 nmol of CNA35-Cy7 (Fig. 1c,d; Supp. Fig. S1d,e). To demonstrate that CNA35 specifically targets collagen in fibrotic kidneys, we injected a Cy7-labeled scrambled version of CNA35. As opposed to CNA35-Cy7, the scrambled probe did not specifically accumulate in fibrotic kidneys and it was cleared equally fast from fibrotic and from healthy kidneys (Fig. 1e). To verify the experimental setup, we confirmed that the expression levels of collagen type I and III in fibrotic kidneys were comparable in all mice included in the analysis (Supp. Fig. S2).

Europe PMC Funders Author Manuscripts

Microscopic confirmation of the collagen-binding specificity of CNA35

To prove the specificity of CNA35 binding to collagen fibers, we performed co-stainings with FITC-labeled CNA35 and different types of collagen on renal tissue sections from healthy and UUO mice. CNA35-FITC showed high co-localization with the scar type collagens I and III in fibrotic mouse kidneys, but overlapped minimally with the basement membrane collagen type IV (Fig. 2a). We validated these findings in kidney biopsy specimens from CKD patients (Supp. Fig. S3). As in murine kidneys, CNA35-FITC was localized in the interstitium and around vessels, mainly co-localizing with collagen type I and III, and hardly with type IV. *Ex vivo* analyses of renal tissues from UUO mice injected with CNA35-FITC at 0.5, 4 and 24 h after i.v. administration confirmed the specificity of the probe, showing significantly stronger accumulation in fibrotic than in healthy kidneys (Fig. 2b-c), and a staining pattern that clearly reflects perivascular binding to fibrillar collagen (Fig. 2d).

Collagen upregulation during renal fibrosis is enhanced in perivascular areas

Given the strong CNA35-FITC accumulation observed in perivascular areas (Fig. 2d), we next quantified vascular alterations and perivascular fibrosis in mice with UUO and I/R. While the lumen of arcuate and interlobular arteries as well as afferent and efferent arterioles was markedly narrowed, the adventitia was significantly thickened by more than 50% due to collagen deposition (Fig. 3a-e). Collagen type III staining of human biopsies from patients with IgA nephropathy confirmed this pronounced perivascular fibrosis, which progressively increased with increasing CKD stage (Fig. 3f).

Discussion

We demonstrate specific and non-invasive assessment of collagen deposition in renal fibrosis using fluorophore-labeled CNA35 and optical imaging. Our data extend previous studies with CNA35 in cardiovascular fibrosis, providing the first proof-of-concept for molecular imaging of collagen content in fibrotic kidneys. *Ex vivo* and histological analyses revealed that CNA35 mainly binds to the fibrillar scar collagens type I and III, which are the main components of the ECM in fibrotic kidneys, whereas only a low degree of co-localization was observed with non-fibrillar type IV collagen in basement membranes, consistent with solid-phase binding assays.[5] Importantly, we found similar co-localization of CNA35 and collagen in murine and in human tissues.

Our ex *vivo* optical imaging, assessing CNA35-FITC distribution after i.v. injection, highlighted a prominent perivascular fibrosis in murine models, supported by our quantitative histological analyses showing significant fibrotic thickening of the arterial adventitia due to collagen deposition during fibrosis, both in mice and in patients. This common and up till now rather neglected feature of renal fibrosis is unlikely mediated by hypertension, since both I/R and UUO models are normotensive. Our findings extend the current concept of perivascular cells as important mediators of renal fibrosis, particularly of Gli1+ cells, which reside in and spread from the arterial adventitia.[8, 9]

CNA35 has two key advantages compared to other probes, such as radiolabeled antibodies, that can be also used to specifically target and image collagen deposition in fibrotic tissues. First, CNA35 is promiscuous in detecting several fibrillary collagens and second, it has an approximately fivefold smaller size, allowing better tissue penetration, in particular in fibrotic lesions. Other small peptide- and indole-based probes have recently been reported for specific non-invasive imaging of pulmonary fibrosis using positron emission tomography (PET).[10, 11] These compounds may also hold significant potential for renal fibrosis staging and treatment monitoring, albeit none have yet been tested in kidneys.

We recently reported non-invasive elastin-specific molecular MRI of kidney fibrosis.[4] Compared to elastin, collagen is much more abundant in fibrotic tissue, making it in principle easier to target. Collagens are also upregulated earlier in the disease course. Conversely, however, the higher baseline abundance of collagens in healthy kidneys and other target tissues may result in higher background. Another major limitation of our study were the low animal numbers, which were based on sample size calculations form our previous studies and were, however, sufficient to show significant results. Further it was impossible to perform and analyze the imaging data in a truly blinded manner, due to the obvious morphological distinction between healthy and fibrotic kidneys as well as the difference in CNA35 signal intensity. In the current study, we have not included experiments measuring different degrees of fibrosis, as we have previously demonstrated to be feasible using elastin imaging.[3] In addition, for a successful translation into the clinic, further contrast agent adaptation is needed before first in human studies, since optical imaging approaches are not suitable in kidney fibrosis.

Our study lays the basis for future systematic experiments defining and optimizing targets, probes and imaging algorithms for translational non-invasive and quantitative diagnosis, staging and treatment monitoring of kidney fibrosis.

Materials and Methods

Information on animal models, human renal samples, histology, immunohistochemistry, and immunofluorescence microscopy are provided as Supplementary Material.

Imaging probes and protocols

CNA35 was produced as described previously[5] and labeled with Cy7 for *in vivo* and with FITC for *ex vivo* optical imaging. A scrambled version of CNA35, i.e. with amino-acid substitution Y175K, rendering it unable to bind to collagen, was used as a control. Hybrid computed tomography–fluorescence molecular tomography (CT-FMT) and fluorescence reflectance imaging (FRI) were performed using an in-house optimized procedures.[12, 13] CT-FMT imaging was done at multiple time points after the i.v. injection of CNA35. The CT-FMT data were analyzed using the Imalytics Preclinical software (Gremse-IT GmbH, Germany).[14] Organ segmentations based on the anatomical CT data, were used to quantify fluorescence signal allocated to kidneys and other organs and expressed as % of the injected dose per cm^3. Organ accumulation was normalized to the total fluorescence intensity measured at 3 h post injection. At the end of the *in vivo* experiment, functional blood vessels

Europe PMC Funders Author Manuscripts

were stained via i.v. injection of rhodamine-labeled lectin (Vector Laboratories, USA), to facilitate fluorescence and two-photon microscopy.

Statistical analysis

All data are presented as mean ± SD. Paired *t*-tests were used to compare fibrotic and contralateral kidneys in one animal. The unpaired *t*-test was used for comparison between two groups. One-way analysis of variance (ANOVA) followed by Bonferroni correction was used for comparing >2 groups. Statistical significance was defined as $p < 0.05$.

Supplementary Material

Refer to Web version on PubMed Central for supplementary material.

Acknowledgements

The authors gratefully acknowledge the technical assistance of Marie Cherelle Timm and Simon Otten in histopathology and Michael Vogt in two-photon microscopy. Image templates provided by Servier Medical Art were employed for preparing the graphical abstract.

Funding

This study was supported by the German Research Foundation (DFG: SFB/TRR57, SFB/TRR219, SFB1066, BO3755/3-1, BO3755/6-1, GR5027/2-1 and RTG2375), the German Ministry of Education and Research (BMBF: STOP-FSGS- 01GM1901A), the European Research Council (ERC: StG-309495 and PoC-813086), the European Union (EU-EFRE: European Fund for Regional Development: I3-STM 0800387), the Interdisciplinary Centre for Clinical Research at RWTH (IZKF K7-3, E7-6 and O3-2), and the RWTH START program (09/15, 124/14 and 152/12).

Literature

1. Djudjaj S, Boor P. Cellular and molecular mechanisms of kidney fibrosis. Mol Aspects Med. 2019; 65:16–36. [PubMed: 29909119]
2. Klinkhammer BM, Goldschmeding R, Floege J, et al. Treatment of Renal Fibrosis-Turning Challenges into Opportunities. Adv Chronic Kidney Dis. 2017; 24:117–129. [PubMed: 28284377]
3. Baues M, Dasgupta A, Ehling J, et al. Fibrosis imaging: Current concepts and future directions. Adv Drug Deliv Rev. 2017; 121:9–26. [PubMed: 29108860]
4. Sun Q, Baues M, Klinkhammer BM, et al. Elastin imaging enables noninvasive staging and treatment monitoring of kidney fibrosis. Sci Transl Med. 2019; 11
5. Krahn KN, Bouten CV, van Tuijl S, et al. Fluorescently labeled collagen binding proteins allow specific visualization of collagen in tissues and live cell culture. Anal Biochem. 2006; 350:177–185. [PubMed: 16476406]
6. Boerboom RA, Krahn KN, Megens RT, et al. High resolution imaging of collagen organisation and synthesis using a versatile collagen specific probe. J Struct Biol. 2007; 159:392–399. [PubMed: 17572104]
7. Chen J, Lee SK, Abd-Elgaliel WR, et al. Assessment of cardiovascular fibrosis using novel fluorescent probes. PLoS One. 2011; 6:e19097. [PubMed: 21533060]
8. Kramann R, Goettsch C, Wongboonsin J, et al. Adventitial MSC-like Cells Are Progenitors of Vascular Smooth Muscle Cells and Drive Vascular Calcification in Chronic Kidney Disease. Cell Stem Cell. 2016; 19:628–642. [PubMed: 27618218]
9. Kramann R, Schneider RK, DiRocco DP, et al. Perivascular Gli1+ progenitors are key contributors to injury-induced organ fibrosis. Cell Stem Cell. 2015; 16:51–66. [PubMed: 25465115]
10. Desogere P, Tapias LF, Hariri LP, et al. Type I collagen-targeted PET probe for pulmonary fibrosis detection and staging in preclinical models. Sci Transl Med. 2017; 9

11. Wahsner J, Desogere P, Abston E, et al. (68)Ga-NODAGA-Indole: An Allysine-Reactive Positron Emission Tomography Probe for Molecular Imaging of Pulmonary Fibrogenesis. J Am Chem Soc. 2019; 141:5593–5596. [PubMed: 30908032]
12. Kunjachan S, Gremse F, Theek B, et al. Noninvasive optical imaging of nanomedicine biodistribution. ACS Nano. 2013; 7:252–262. [PubMed: 23067565]
13. Gremse F, Doleschel D, Zafarnia S, et al. Hybrid microCT-FMT imaging and image analysis. J Vis Exp. 2015:e52770. [PubMed: 26066033]
14. Gremse F, Stark M, Ehling J, et al. Imalytics Preclinical: Interactive Analysis of Biomedical Volume Data. Theranostics. 2016; 6:328–341. [PubMed: 26909109]

Europe PMC Funders Author Manuscripts

Europe PMC Funders Author Manuscripts

Translational Statement

The pathological correlate of chronic kidney disease is renal fibrosis, i.e. deposition of extracellular matrix, in particular collagen. Here we introduced molecular imaging for noninvasive visualization and quantification of collagen deposition in murine renal fibrosis models using the collagen binding molecular probe CNA35 in combination with hybrid computed tomography fluorescence molecular tomography imaging. For translation into clinical use, further probe and protocol optimization will be required. The final goal is to establish non-invasive diagnostic methods to specifically monitor and quantify kidney fibrosis, to provide novel endpoints for clinical trials and to improve the management of CKD patients.

Europe PMC Funders Author Manuscripts

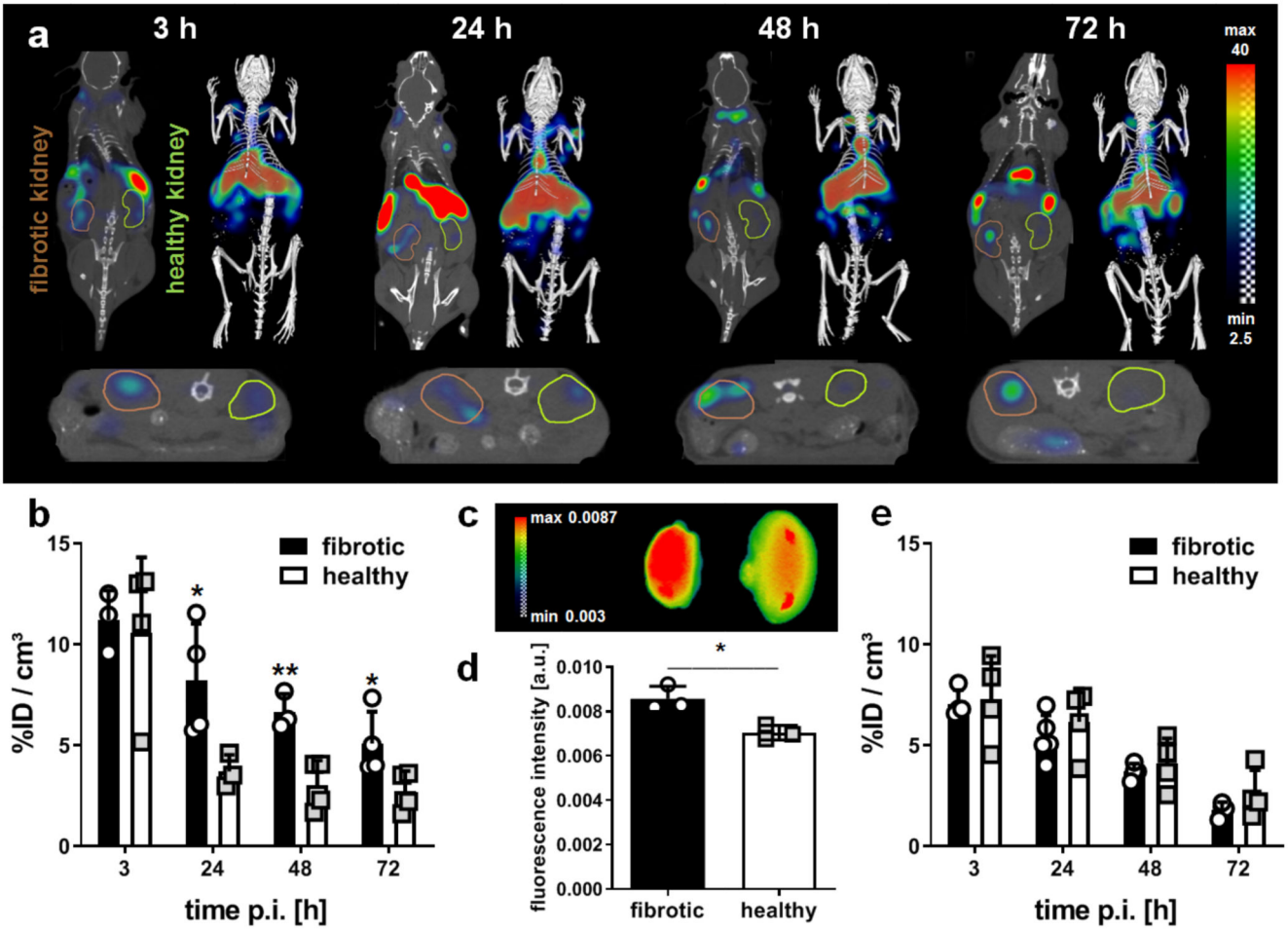

Figure 1. ***In vivo*** **and** ***ex vivo*** **optical imaging of collagen deposition kidneys with I/R-induced fibrosis using CNA35-Cy7.**

(a) Coronal (left) and transversal (bottom) slices as well as 3D renderings (right) for hybrid computed tomography-fluorescence molecular tomography (CT-FMT) imaging of CNA35 biodistribution in a mouse with I/R-induced renal fibrosis at different time points after the i.v. injection of 1 nmol CNA35-Cy7. The fibrotic kidney is encircled in brown (left) and the healthy kidney in green (right) in the coronal view. **(b)** Quantification of the *in vivo* CT-FMT images shows prominent accumulation of CNA35-Cy7 in fibrotic kidneys at 24, 48 and 72 h after probe administration. **(c, d)** *Ex vivo* fluorescence reflectance imaging (FRI) at 72 h post injection confirms higher CNA35 accumulation in fibrotic kidneys (left). **(e)** Quantification of the kidney accumulation of scrambled CNA35-Cy7, demonstrating no specific accumulation in fibrotic vs. healthy kidneys. Values represent mean ± SD based on quantifying n=4 mice. *p<0.05, **p<0.01.

Europe PMC Funders Author Manuscripts

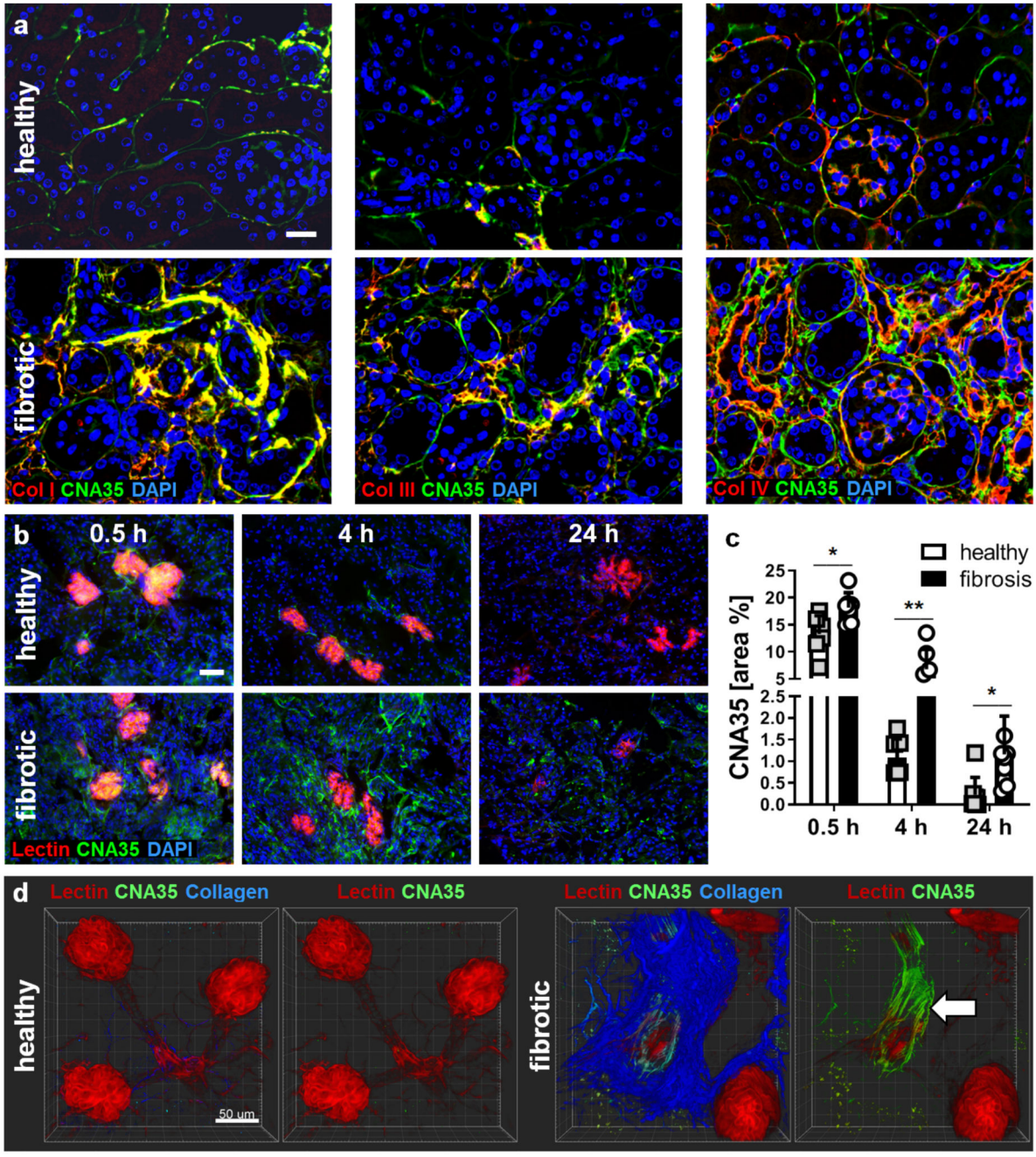

Figure 2. Microscopy imaging of collagen deposition in fibrotic kidneys using CNA35-FITC.

(a) Fluorescence microscopy analysis showing the co-localization of FITC-labeled CNA35 (green; upon incubation of tissue sections) with collagen fibers of type I, III and IV (all in red) on renal tissue sections from healthy mice and UUO mice. Nuclei are counterstained using DAPI (blue). Scale bar: 50 μm. **(b)** Representative immunofluorescence images showing the accumulation of FITC-labeled CNA35 (green) in healthy and fibrotic kidneys at 0.5, 4 and 24 h after i.v. injection. Perfused blood vessels are counterstained using rhodamine-lectin (red), cell nuclei using DAPI (blue). Scale bar: 50 μm. **(c)** Quantification

of CNA35-FITC accumulation in fibrotic vs. healthy kidneys upon i.v. injection. **(d)** Two-photon laser scanning microscopy (TPLSM) indicated specific co-localization with collagen fibers (visualized using second harmonic generation) and much stronger enrichment of CNA35-FITC in fibrotic kidneys than in contralateral healthy kidneys, particularly around blood vessels (arrow). Scale bar: 50 μm. Values represent mean ± SD based on n=6 sections. *p<0.05, **p<0.01.

Europe PMC Funders Author Manuscripts

Europe PMC Funders Author Manuscripts

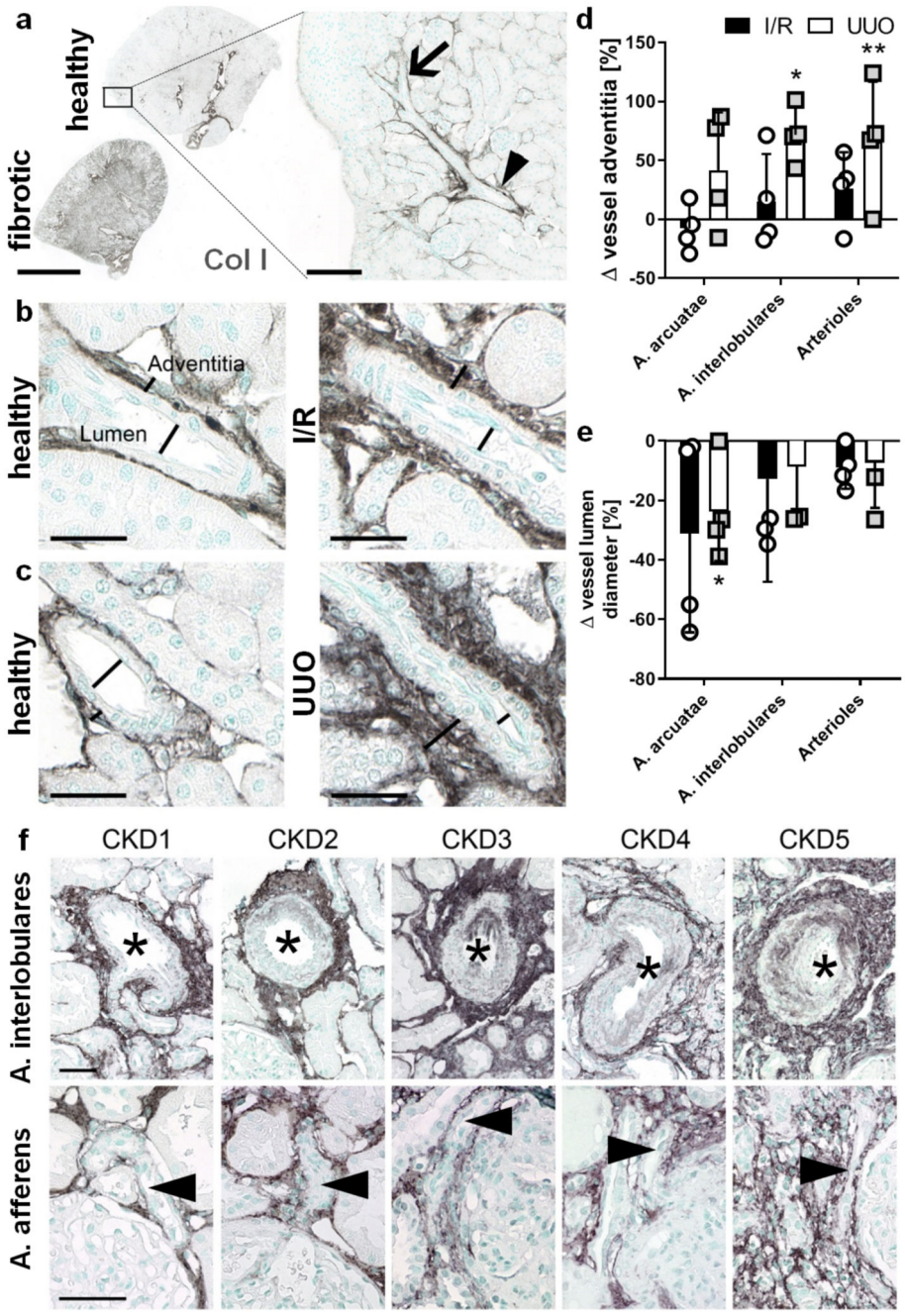

Figure 3. Perivascular fibrosis is a constant feature of renal fibrosis in animal models and patients.

(a) Localization and expression of collagen I in healthy and fibrotic renal tissue. The arrowhead points at the arteria arcuatae and the arrow indicates the arteria interlobulares. Scale bar: 2 mm. **(b-e)** Collagen type I is upregulated during renal fibrosis in both I/R **(b)** and UUO **(c)** not only in the interstitium, but also in the thickened adventitia of arterial vessels **(d).** Vessels showed a reduced vessel lumen diameter throughout the entire renal artery branches **(e).** Scale bar: 25 μm. **(f)** Enhanced collagen type III deposition in

perivascular areas was also a common feature in human biopsies and increased with increasing CKD stage. The asterisks indicate the vessel lumen of arteria interlobulares and the arrowheads mark arteria afferens. Scale bar: 50 μm. Values represent mean ± SD based on quantifying n=4 mice per group. *p<0.05, **p<0.01 fibrotic vs. healthy kidney.

Europe PMC Funders Author Manuscripts